Biochimica et Biophysica Acta 1797 (2010) 945–951

Contents lists available at ScienceDirect

Biochimica et Biophysica Acta

journal homepage: www.elsevier.com/locate/bbabio

The p13 protein of human T cell leukemia virus type 1 (HTLV-1) modulates mitochondrial membrane potential and calcium uptake

Roberta Biasiotto [a], Paola Aguiari [b], Rosario Rizzuto [c], Paolo Pinton [b], Donna M. D'Agostino [a,d], Vincenzo Ciminale [a,d,*]

[a] Department of Oncology and Surgical Sciences, University of Padova, I-35128 Padova, Italy
[b] Department Experimental and Diagnostic Medicine, Section of General Pathology, Interdisciplinary Center for the Study of Inflammation (ICSI) and Emilia Romagna Laboratory BioPharmaNet, University of Ferrara, I-44100 Ferrara, Italy
[c] Department of Biomedical Sciences, University of Padova, I-35100 Padova, Italy
[d] Istituto Oncologico Veneto-IRCCS, Padova, Italy

ARTICLE INFO

Article history:
Received 16 November 2009
Received in revised form 18 February 2010
Accepted 19 February 2010
Available online 25 February 2010

Keywords:
Mitochondria
Viroporin
Membrane potential
Calcium homeostasis
HTLV-1
Potassium channel

ABSTRACT

Human T cell leukemia virus type 1 (HTLV-1) encodes p13, an 87-amino-acid protein that accumulates in the inner mitochondrial membrane. Recent studies performed using synthetic p13 and isolated mitochondria demonstrated that the protein triggers an inward potassium (K^+) current and inner membrane depolarization. The present study investigated the effects of p13 on mitochondrial inner membrane potential ($\Delta\psi$) in living cells. Using the potential-dependent probe tetramethyl rhodamine methyl ester (TMRM), we observed that p13 induced dose-dependent mitochondrial depolarization in HeLa cells. This effect was abolished upon mutation of 4 arginines in p13's α-helical domain that were previously shown to be essential for its activity in *in vitro* assays. As $\Delta\psi$ is known to control mitochondrial calcium (Ca^{2+}) uptake, we next analyzed the effect of p13 on Ca^{2+} homeostasis. Experiments carried out in HeLa cells expressing p13 and organelle-targeted aequorins revealed that the protein specifically reduced mitochondrial Ca^{2+} uptake. These observations suggest that p13 might control key processes regulated through Ca^{2+} signaling such as activation and death of T cells, the major targets of HTLV-1 infection.

1. Introduction

Human T cell leukemia virus type 1 (HTLV-1) is a retrovirus that infects 10–20 million people worldwide. Although most persons infected with HTLV-1 remain life-long asymptomatic carriers, about 3–5% eventually develop adult T cell leukemia/lymphoma (ATLL), an aggressive neoplasm of mature CD4+ T cells, or tropical spastic paraparesis/HTLV-associated myelopathy (TSP/HAM), a progressive demyelinating disease that mainly targets the thoracic spinal cord [1,2].

In addition to the *gag*, *pol*, and *env* genes found in all retroviruses, the HTLV-1 genome contains other open reading frames coding for the regulatory proteins Tax and Rex, both of which are essential for viral replication, and accessory proteins named p12, p21, p30, HBZ, and p13 [3]. Detailed studies of the oncogenic potential of HTLV-1 have identified Tax as a major factor driving transformation. In addition to activating transcription from the viral promoter, Tax affects the expression of cellular genes controlling cell proliferation, apoptosis, and chromosomal stability and is sufficient for immortalization of T cells [4]. However, the low prevalence and long latency of ATLL (usually several decades from infection to diagnosis) indicate that additional viral and cellular factors must influence the balance between persistent, disease-free infection and Tax-driven leukemogenesis.

The present study is focused on the viral accessory protein p13. Initial studies of p13 demonstrated that it accumulates in mitochondria and disrupts mitochondrial morphology, resulting in isolated clusters of round-shaped, apparently swollen mitochondria, some of which form ring-like structures [5,6]. Cells expressing p13 exhibit reduced proliferation rates and increased sensitivity to apoptosis triggered by ceramide and FasL [7,8]. p13 also interferes with the ability of HeLa cells and Ras/Myc-transformed primary fibroblasts to grow as tumors in nude mice, suggesting that it may exert tumor-suppressor-like activity [8].

Immunoelectron microscopy and fractionation experiments demonstrated that p13 is an integral membrane protein and accumulates mainly in the inner mitochondrial membrane [9]. Its 87-amino-acid sequence includes a mitochondrial targeting signal (MTS) spanning amino acids 21–31 [5] that contains 4 arginines. Although p13 mutants carrying substitutions of the arginines with glutamines, prolines, or alanines and leucines retain mitochondrial targeting, they produce little or no mitochondrial fragmentation/swelling, indicating

* Corresponding author. Dipartimento di Scienze, Oncologiche e Chirurgiche, Via Gattamelata 64, 35128 Padova, Italy. Tel.: +39 049 821 5885; fax: +39 049 807 2854.
E-mail address: v.ciminale@unipd.it (V. Ciminale).

0005-2728/$ – see front matter © 2010 Elsevier B.V. All rights reserved.
doi:10.1016/j.bbabio.2010.02.023

that the are essential for these effects [9]. The MTS of p13 (LRVWRLCTRRL) is predicted to form an α-helix, with the 4 arginines forming a positively charged face, thereby imparting amphipathic properties to this region [9]. Biophysical and biochemical analyses of a synthetic peptide spanning residues 9–41 ($p13^{9-41}$) confirmed that this region folds into an amphipathic α-helix upon exposure to membrane-mimetic solutions [9]. Initial *in vitro* assays carried out using isolated rat liver mitochondria and $p13^{9-41}$ demonstrated that the peptide induced energy-dependent swelling that depended on K^+ and mitochondrial inner membrane potential ($\Delta\psi$). These effects were evident when the peptide was used in the low micromolar range and required the presence of the critical arginine residues [9]. More recent analyses of full-length synthetic p13 revealed that it is at least 10-fold more potent than $p13^{9-41}$ in changing K^+ permeability in isolated mitochondria. In these assays, p13 induced an influx of K^+ into the mitochondrial matrix; this effect was evident using as little as 50–100 nM of the protein and was lost upon collapse of $\Delta\psi$ with carbonylcyanide *p*-trifluoromethoxyphenylhydrazone (FCCP). Increased K^+ permeability was accompanied by a dose-dependent reduction in $\Delta\psi$. In addition, the protein induced an increase in respiratory chain activity, which partially masked its effects on $\Delta\psi$ while augmenting production of reactive oxygen species (ROS). The protein also reduced the threshold for permeability transition pore (PTP) opening [10]. The effects of p13 on $\Delta\psi$, respiratory chain activity, ROS production, and sensitization to PTP opening were evident at doses of 100–200 nM. The present study extends these *in vitro* findings by testing the effects of p13 on $\Delta\psi$ in living cells. Results confirm that p13 exerts a dose-dependent effect on $\Delta\psi$ leading to a reduction in mitochondrial Ca^{2+} uptake.

2. Materials and methods

2.1. Plasmids

Plasmid pSGp13, expressing p13 under the control of the SV40 promoter, and derivatives in which arginines at positions 22, 25, 29, and 30 were mutated either to glutamines (pSGp13RQ), alanine–leucine–leucine–alanine (pSGp13RAL), or prolines (pSGp13RP), were previously described [9]. pcDNAp13–GFP, expressing p13 fused to enhanced green fluorescent protein, was constructed by inserting the fused gene into the CMV promoter-driven vector pcDNA3.1 (Invitrogen). pcDNAp13RQ–GFP, containing glutamines instead of arginines as described for pSGp13, was generated by PCR-based plasmid mutagenesis (Quikchange, Stratagene). Plasmids expressing chimeric aequorins targeted to mitochondria (mtAEQmut), the cytosol (cytAEQ), and the endoplasmic reticulum (ER; erAEQmut) were previously described [11]; "AEQ" refers to wild-type aequorin, and "AEQmut" refers to a low-affinity D119A mutant of aequorin.

2.2. Analysis of $\Delta\psi$

Membrane potential experiments utilized the HeLa-derived cell line HeLa-Tat, selected for its high transfection efficiency [12]. The cells were maintained in Dulbecco's modified Eagle's medium (Sigma) supplemented with 10% fetal calf serum (FCS; Invitrogen), 100 U/ml penicillin, and 20 U/ml streptomycin (complete DMEM). Cells were seeded at a density of 75,000 cells/ml onto 35-mm plates, cultured for 24 h, and then transfected with a plasmid expressing either wild-type p13WT–GFP or mutant p13RQ–GFP using Fugene 6 reagent (Roche). Eighteen hours after transfection, the cells were incubated with 5 nM tetramethyl rhodamine methyl ester (TMRM, Molecular Probes) for 30 min at 37 °C in the presence of 20 μg/ml verapamil (Sigma) to block activity of the multidrug resistance pump and allow efficient and uniform TMRM loading [13,14]. Culture plates were transferred to a 37 °C, 5% CO_2 incubator attached to a Zeiss LSM510 laser scanning microscope. Images of the living cells were obtained using a helium neon (543 nm) laser to excite TMRM and an argon laser (488 nm) to excite GFP; laser intensity, pinhole aperture, and photomultiplier parameters were standardized to allow comparable measurements.

The mean fluorescence intensities of GFP and TMRM of individual cells were quantitated using the Zeiss "Histogram" software tool. At least 100 cells from 4 different randomly selected fields were measured for each experimental group. Expression levels of GFP-fusion proteins from 4 independent experiments were normalized to the respective mean value of fluorescence intensity of p13–GFP, while the mitochondrial membrane potential values were normalized to the respective mean value of TMRM fluorescence intensity in control non-transfected cells. The normalized GFP fluorescence intensity values were used to separate cells into 5 groups with different levels of p13 expression; mean TMRM fluorescence values in these expression groups were plotted. Statistical analysis was carried out using the Student's *t*-test.

2.3. Analysis of the mitochondrial localization of p13

HeLa-Tat cells were seeded at a density of 75,000 cells/ml onto 35-mm plates, cultured for 24 h, and then transfected with a pSG plasmid expressing either wild-type (pSGp13) or mutant (pSGp13RQ) p13 using Fugene 6 reagent (Roche). Twenty-four hours after transfection, the cells were washed in DMEM and fixed in 3.7% formaldehyde in complete DMEM for 20 min. Cells were permeabilized in 0.1% Nonidet P-40-PBS for 10 min, washed twice with PBS, and incubated for 45 min at 37 °C with rabbit polyclonal anti-p13 and goat anti-Hsp60 (Santa Cruz), a mitochondrial protein used as marker of mitochondrial localization. After two washes with PBS, cells were incubated for 30 min at 37 °C with Alexa 488-conjugated anti-rabbit antibody and Alexa 546-conjugated anti-goat antibody (Molecular Probes). After two washes with PBS, fluorescent signals were analyzed by laser scanning microscopy using argon (488 nm) and helium neon (543 nm) lasers sources to excite the Alexa 488 and Alexa 646 fluorochromes, respectively. Images were taken with a 63× objective at an optical slice of 1 μm. Approximately 30 cells from 4 different randomly selected fields were measured for each experimental group. Expression levels of p13 proteins from 2 independent experiments were normalized to the respective mean value of fluorescence intensity of p13. By using the Zeiss Histogram software, the colocalization indexes between the two signals (which are detected in channels 1 and 2 for Hsp60 and p13, respectively) were calculated for single cells. The colocalization index 1 (CI1) expresses a measure of the mitochondrial "filling" with p13 and is the relative number of the colocalizing p13-Hsp60 pixels, as compared to the total number of Hsp60 pixels above threshold. Colocalization index 2 (CI2), which indicates the mitochondrial localization of p13, is the ratio between the colocalizing p13-Hsp60 pixels and the total number of p13 pixels above threshold. The CI values can range between 0 and 1, according to increasing levels of colocalization between the pixels of the two channels (channel 1 = Hsp60, channel 2 = p13; CI = 0 = no colocalization; CI = 1 = 100% colocalization). CI1 and CI2 were calculated according to the following formulas: $CI1 = pixels_{Ch1coloc}/pixels_{Ch11total}$; $CI2 = pixels_{Ch2coloc}/pixels_{Ch2total}$. The normalized p13 fluorescence intensity values were used to separate cells into 4 groups with different levels of p13 expression; mean CI values in these expression groups were plotted on the *y*-axis. Statistical analysis was carried out using the Student's *t*-test.

2.4. Analysis of Ca^{2+} homeostasis

HeLa cells, maintained in complete DMEM, were seeded onto 13-mm glass coverslips, grown to 50% confluence, and transfected by calcium phosphate coprecipitation. Transfection mixtures contained 3 μg of a pSGp13 plasmid expressing wild-type or mutant p13 or a control plasmid expressing mitochondrial-targeted GFP (mtGFP [15]) and 1 μg of a plasmid expressing mtAEQmut, cytAEQ, or erAEQmut. For cytosolic and mitochondrial Ca^{2+} measurements, transfected HeLa cells were incubated with 5 μM coelenterazine for 1.5 h in

DMEM supplemented with 1% FCS and transferred to the luminometer perfusion chamber. To efficiently reconstitute erAEQmut, the luminal [Ca^{2+}] of the ER was reduced by incubating cells for 1 h at 4 °C in modified Krebs-Ringer Buffer (KRB, containing 125 mM NaCl, 5 mM KCl, 1 mM $MgSO_4$, 1 mM Na_2HPO_4, 5.5 mM glucose, and 20 mM HEPES) supplemented with 5 μM coelenterazine, 5 μM ionomycin (Sigma), and 600 μM EGTA. Cells were then extensively washed with KRB supplemented with 2% bovine serum albumin (BSA) and 1 mM EGTA and transferred to the luminometer perfusion chamber. All aequorin measurements were performed in KRB supplemented with 1 mM $CaCl_2$. Histamine (100 μM) was used as an agonist. To discharge the residual aequorin pool and calibrate the signal, cells were lysed with 100 μM digitonin in a hypotonic Ca^{2+}-rich solution (10 mM $CaCl_2$ in H_2O). The aequorin luminescence data were converted to [Ca^{2+}] values using a computer algorithm based on the Ca^{2+} response curve of wild-type and mutant aequorins as described previously [11]. Results were expressed as means ± standard error and analyzed for statistical significance using the Student's *t*-test.

3. Results and discussion

3.1. Effects of p13 on Δψ

In previous studies carried out using isolated mitochondria, we demonstrated that p13 induces a K^+ influx resulting in depolarization and increased ROS production; these alterations in turn lower the opening threshold of the permeability transition pore [10]. These effects were dependent on the presence of four arginines (22, 25, 29, and 30) in the functional α-helical domain spanning amino acids 21–31 [9,10].

In the present work, we tested the effects of p13 in living cells by employing plasmids expressing GFP-tagged wild-type p13 (p13WT–GFP) or a mutant of p13 in which the critical arginines were substituted with glutamines (p13RQ–GFP). Δψ was measured using tetramethyl rhodamine methyl ester (TMRM), a fluorescent lipophilic cation that accumulates in the mitochondrial matrix in a Δψ-dependent manner. The fluorescence intensity of TMRM in individual p13-expressing cells (i.e., those with a GFP signal) was measured using laser scanning microscopy. To confirm the potential-dependent staining of TMRM, cells were incubated with 1 μM FCCP, a protonophore that collapses the Δψ. This treatment resulted in a loss of TMRM fluorescence, thus confirming the probe's dependence on Δψ and indicating that the assay was carried out below its quenching threshold (data not shown).

Fig. 1 shows a quantitative analysis of the effects of p13 on Δψ in cells expressing various levels of the protein, measured as GFP fluorescence intensity: panels A and B show TMRM-labeled cells with low-intermediate levels of p13WT–GFP and p13RQ–GFP, respectively, and panels C and D show cells expressing higher levels of the proteins. The tables on the right-hand side of the figure report the mean fluorescence intensities of GFP and TMRM in all the cells analyzed in the images (indicated by numbers). The scatter plots show TMRM fluorescence intensity (*y*-axis) and GFP fluorescence intensity (*x*-axis) measured within a single cell, indicated by a white line. Cells expressing low to intermediate levels of p13WT–GFP varied in terms of Δψ, while cells expressing p13RQ–GFP invariably maintained Δψ (see tables in panels A and B); these observations indicated that p13 was essential but not sufficient for depolarization and suggested that its function might be subjected to regulation. Future studies will be aimed at investigating this possibility. In contrast, cells expressing high levels of p13WT–GFP (panel C) exhibited a marked reduction in TMRM. No reduction in TMRM fluorescence was observed in cells expressing high levels of p13RQ–GFP (panel D).

The effect of p13–GFP on Δψ in living cells was further analyzed using data collected from 4 independent experiments, with at least 100 cells expressing p13WT–GFP or p13RQ–GFP at different levels analyzed in each experiment. TMRM signals measured in cells expressing p13WT–GFP or p13RQ–GFP were scaled against the mean TMRM fluorescence intensity measured in non-transfected cells (i.e., cells without a detectable GFP signal), and fluorescence intensity values measured for p13RQ–GFP were scaled against the mean fluorescence intensity of p13WT–GFP.

In Fig. 2A, normalized GFP fluorescence intensity values were used to separate cells into 5 groups with different levels of p13 expression, and mean TMRM fluorescence values for each group were plotted. This analysis revealed that cells expressing lower levels of p13WT–GFP exhibited mean Δψ values similar to those recorded in cells expressing comparable levels of p13RQ–GFP. However, as p13 expression levels increased, Δψ progressively diminished. In contrast, no significant change in Δψ was observed as p13RQ–GFP levels increased. Statistical analysis demonstrated highly significant differences in Δψ between wild-type and mutant p13 expressing cells in the intermediate (1.5–1.99 expression group; $p = 0.0063$) and high expression groups (≥2 expression group; $p = 2.92 \times 10^{-6}$).

As shown in Fig. 2B, the mean values of TMRM fluorescence of the wild-type vs. mutant p13-expressing cells were significantly different even after pooling all data irrespective of expression levels ($p = 4.28 \times 10^{-5}$). The mean expression level of p13RQ–GFP was slightly lower than that of p13WT–GFP, but this difference was not statistically significant (data not shown).

Taken together, these observations indicated that the effect of p13 on Δψ in living cells might be dose-dependent as observed in previous assays carried out using synthetic p13 and isolated mitochondria [10].

3.2. Intracellular targeting of WT vs. mutant p13

To determine whether the lack of effect of p13RQ–GFP expression on Δψ might be due to defective mitochondrial targeting compared to the wild-type protein, we analyzed the colocalization of p13WT and p13RQ with Hsp60 used as a marker of the mitochondrial compartment (Fig. 3). Results were analyzed by calculating "colocalization indexes" (CI) indicating the fraction of the p13 (wild-type or mutant) localized in mitochondria (CI2, panel A) and the fraction of mitochondrial pixels (i.e., Hsp60) that are also positive for p13 (CI1, panel B). Results showed that the mutant p13RQ was more efficiently targeted to mitochondria than p13WT (panel A) and that the mitochondrial compartment presented a similar "filling" with p13RQ compared to p13WT (panel B), suggesting that the lack of effect of p13RQ on Δψ was not due to a reduced mitochondrial targeting. As shown in Fig. 3C, the overall expression levels of wild-type vs. mutant p13 were comparable.

3.3. Effects of p13 on Ca^{2+} uptake by mitochondria

Δψ drives mitochondrial uptake of Ca^{2+} through the Ca^{2+} uniporter, a high-affinity Ca^{2+} channel located in the inner membrane [16] and/or via the 'rapid uptake mode' [17]. Ca^{2+} uptake by mitochondria spatially and temporally confines elevated cytosolic Ca^{2+} concentrations, which arise through mobilization of Ca^{2+} from the endoplasmic reticulum (ER) via triggering of the IP3 and ryanodine receptors and by entry from the extracellular medium through plasma membrane channels. The amplitude, number, and duration of cytosolic Ca^{2+} transients constitute a complex signaling pathway that controls a vast number of biological responses ranging from muscle contraction to secretion, control of transcription, and apoptosis. As mitochondrial Ca^{2+} uptake is known to be driven by Δψ [18], we next investigated whether p13-induced mitochondrial depolarization affects mitochondrial Ca^{2+} homeostasis. This was tested by transfecting HeLa cells with wild-type p13, a panel of p13 arginine mutants (p13RQ, p13RP, p13RAL), or mitochondrial-targeted GFP (serving as a control mitochondrial protein) together with an aequorin probe targeted to the mitochondria. After aequorin

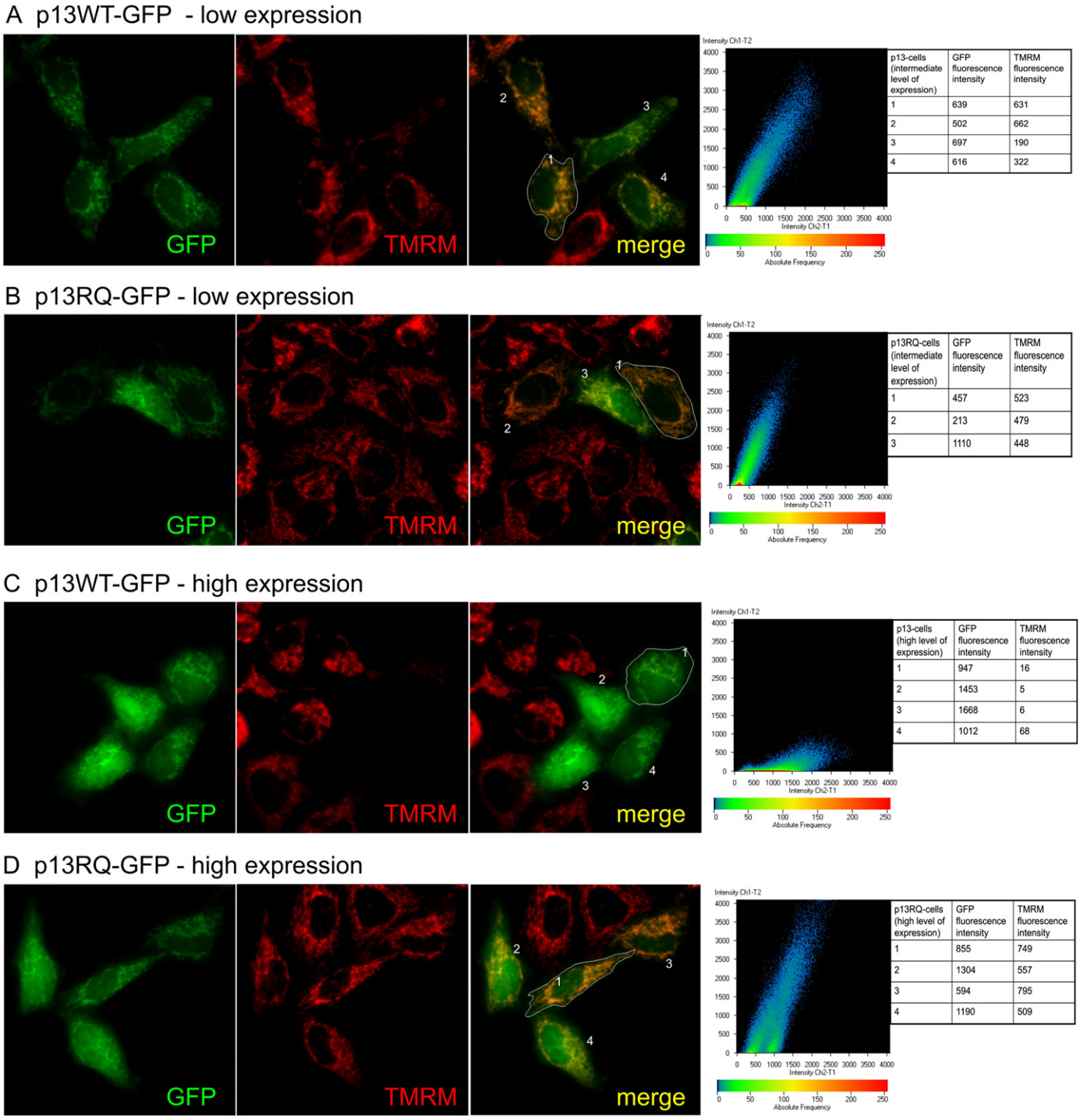

Fig. 1. Effects of p13 on $\Delta\psi$ in cells. HeLa-Tat cells were transfected with p13WT–GFP or p13RQ–GFP. Eighteen hours later, cells were incubated with 5 nM TMRM and 20 μg/ml verapamil for 30 min, and fluorescence intensities of TMRM and GFP were detected by laser scanning microscopy and analyzed as described in Materials and methods. Images show the GFP, TMRM, and overlay signals (20× magnification). The scatter plot shows TMRM fluorescence intensity plotted against GFP fluorescence intensity measured in the cell selected by the white line. Tables report GFP and TMRM fluorescence measured in the numbered cells.

reconstitution, cells were challenged with 100 μM histamine, an agonist that acts on G-coupled receptor resulting in inositol 1,4,5 triphosphate (IP3) production and Ca^{2+} release from intracellular stores. This assay was performed 3 times, with results assessed by measuring the Ca^{2+} peak amplitude.

As shown in Fig. 4A, p13WT caused a mean 56% reduction in the mitochondrial Ca^{2+} peak amplitude compared to the control (peak amplitude: p13WT = 27 ± 4 μM; control = 62 ± 3 μM; $p = 3 \times 10^{-6}$). In contrast, the arginine mutants p13RQ and p13RAL did not significantly affect mitochondrial Ca^{2+} uptake (peak amplitude: p13RQ = 69 ± 4 μM; p13RAL = 63 ± 4 μM). p13RP produced a modest but statistically significant increase in mitochondrial Ca^{2+} content (peak amplitude: p13RP = 74 ± 5 μM, $p = 0.04$).

To investigate whether p13's effects on mitochondrial Ca^{2+} content could also influence cytosolic [Ca^{2+}] or could be dependent on a change in Ca^{2+} release from the ER, we measured the effects of p13 on cytosolic and ER [Ca^{2+}] using aequorins targeted to these compartments. Results of 3 independent experiments showed that

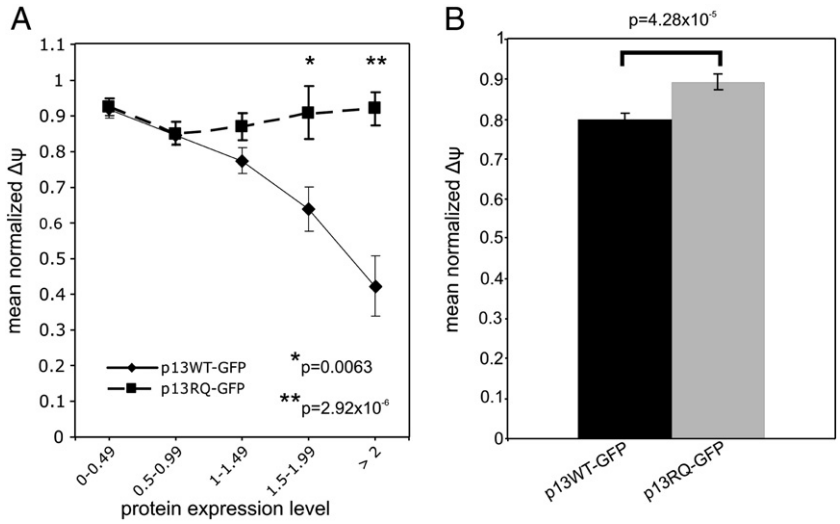

Fig. 2. $\Delta\psi$ in p13-expressing cells. Panel A shows TMRM fluorescence plotted against p13 expression ranges, normalized as indicated in Materials and methods. The data were obtained from the analysis of 487 p13WT–GFP and 409 p13RQ–GFP cells. The asterisks indicate a significant difference calculated by the Student's *t*-test. In protein expression level group 0–0.49, $p = 0.8222$; group 0.5–1, $p = 0.8942$; group 1–1.5, $p = 0.0744$; group 1.5–1.99, $p = 0.0063$, and group >2 = 2.926×10^{-6}. The plot in panel B was generated with data pooled from all analyzed cells. $\Delta\psi$ is represented as the ratio between the fluorescence intensity (FI) of TMRM in p13WT- or p13RQ-expressing cells and the TMRM mean fluorescence intensity in non-transfected cells. Mean normalized values and standard error bars are reported. $p = 4.28 \times 10^{-5}$ (Student's *t*-test).

p13WT did not significantly affect cytosolic [Ca^{2+}] (Fig. 4B, peak amplitudes: control = 2.37 ± 0.07 μM; p13WT = 2.30 ± 0.12 μM; p13RQ = 2.54 ± 0.06 μM; p13RP = 2.40 ± 0.10 μM; p13RAL = 2.22 ± 0.09 μM). Wild-type p13 and the arginine mutants p13RP and p13RAL did not substantially alter ER Ca^{2+} filling (Fig. 4C, steady state: control = 442 ± 13 μM; p13WT = 460 ± 27 μM; p13RP = 500 ± 20 μM; p13RAL = 489 ± 18 μM), while the glutamine mutant induced slightly higher ER loading compared to the control (steady state: p13RQ = 520 ± 20 μM, $p = 0.01$).

As depicted in the model in Fig. 5, these results demonstrate that p13 specifically reduces mitochondrial Ca^{2+} uptake; the observation that the arginine mutants did not influence mitochondrial Ca^{2+} uptake strongly suggests that this effect is tightly linked to the ability of p13 to induce mitochondrial K^+ influx and depolarization. The fact that p13 did not induce a significant overall change in cytosolic Ca^{2+} concentration suggests that mitochondrial depolarization may influence cytosolic Ca^{2+} concentration only locally. It would be interesting to determine whether p13 affects Ca^{2+} concentration in close vicinity to plasma membrane Ca^{2+} channels. In this case, p13 may influence store-operated calcium entry, which is of a crucial importance during T cell activation. It is also possible that p13's effects on Ca^{2+} homeostasis might result from the protein's ability to promote mitochondrial fragmentation [5].

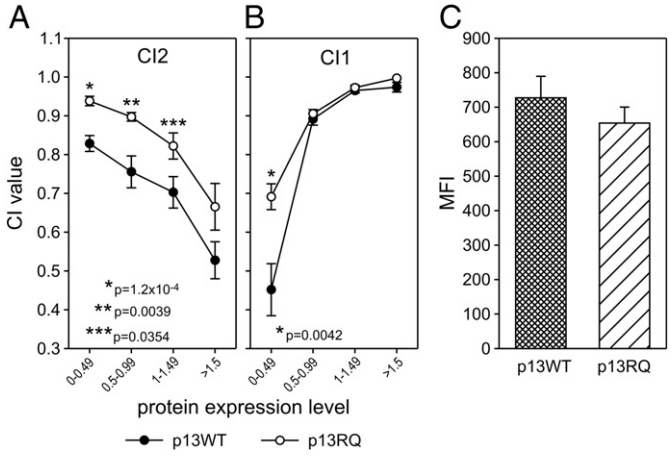

Fig. 3. Mitochondrial targeting of p13WT and p13RQ. Graphs represent colocalization indexes CI2 (A) and CI1 (B) as a function of p13 expression levels, calculated as indicated in Materials and methods. Data were derived from the analysis of 56 and 61 cells expressing p13WT and p13RQ, respectively, from 2 independent experiments. Asterisks indicate a significant difference between the wild-type and the mutant in the corresponding expression level calculated using Student's *t*-test. Mean normalized values and standard error bars are indicated. In panel A, in protein expression level group 0–0.49, $p = 1.2 \times 10^{-4}$; group 0.5–0.99, $p = 0.0039$; group 1–1.49, $p = 0.0354$; group >1.5, $p = 0.0896$. In panel B, in protein expression level group 0–0.49, $p = 0.0042$; group 0.5–0.99, $p = 0.4732$; group 1–1.49, $p = 0.4294$; group >1.5, $p = 0.0828$. In panel C, $p = 0.3484$.

Modulation of Ca^{2+} signaling pathways is a common mechanism employed by viruses to maximize dissemination and persistence of infection, with impingement occurring either through direct binding to Ca^{2+}, modification of membrane permeability, or alteration of the activity of individual signaling components (e.g., channels, pumps, chaperones, Ca^{2+} sensors, transcription factors) [19,20].

The effects of p13 on Ca^{2+} signaling could be particularly relevant in the context of T cells, the natural target of HTLV-1 infection, as functional mitochondria are essential for efficient activation through engagement of the T cell receptor complex [21–23]. Mitochondria could also play a role during cell-to-cell transmission of HTLV-1 through the "virological synapse", as it was recently demonstrated that mitochondria are redistributed to the contact points between the infected 'donor' cell and the target cell [24]. This possibility would be consistent with the finding that p13 is essential for viral propagation *in vivo*, as suggested by results of studies in a rabbit model [25]. The results of the Ca^{2+} uptake assays provide a mechanistic explanation for the effect of p13 on Ca^{2+}-dependent CREB phosphorylation reported in a previous study [8]. Consistent with these findings, HTLV-1 infection was shown to lead to an alteration in intracellular Ca^{2+} levels leading to changes in the expression of Ca^{2+}-related genes [26].

p13's ability to increase mitochondrial K^+ permeability and in turn influence mitochondrial $\Delta\psi$ and Ca^{2+} homeostasis depends on the integrity of its amphipathic α-helix. This property, together with its propensity to form high-molecular weight complexes [9], suggests that p13 may function as a viroporin. Viroporins are small viral proteins that contain transmembrane amphipathic α-helical domains whose multimerization in the context of membranes results in the formation of channel-like structures. One interesting example of a viroporin is p7 of hepatitis C virus (HCV), a 63-amino-acid protein that accumulates primarily in the ER [27]. p7 is necessary for both

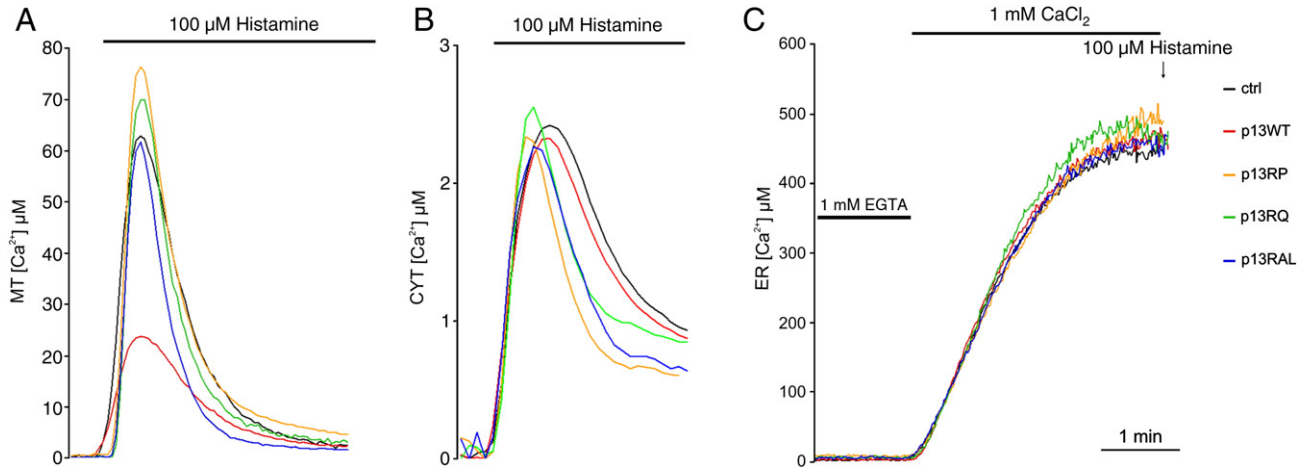

Fig. 4. Measurement of Ca^{2+} content in mitochondria (MT), cytosol (CYT), and endoplasmic reticulum (ER) of p13-expressing cells. $[Ca^{2+}]$ in mitochondria (A), cytosol (B), and endoplasmic reticulum (C) of HeLa cells expressing control (mtGFP), p13WT, or p13-arginine mutants (p13RQ, p13RP, p13RAL) was analyzed using aequorin probes as described in Materials and methods. After aequorin reconstitution, cells were challenged with 100 μM histamine, as indicated in the graphs. The traces show resulting measurements of $[Ca^{2+}]$ as a function of time and are representative of 3 independent experiments.

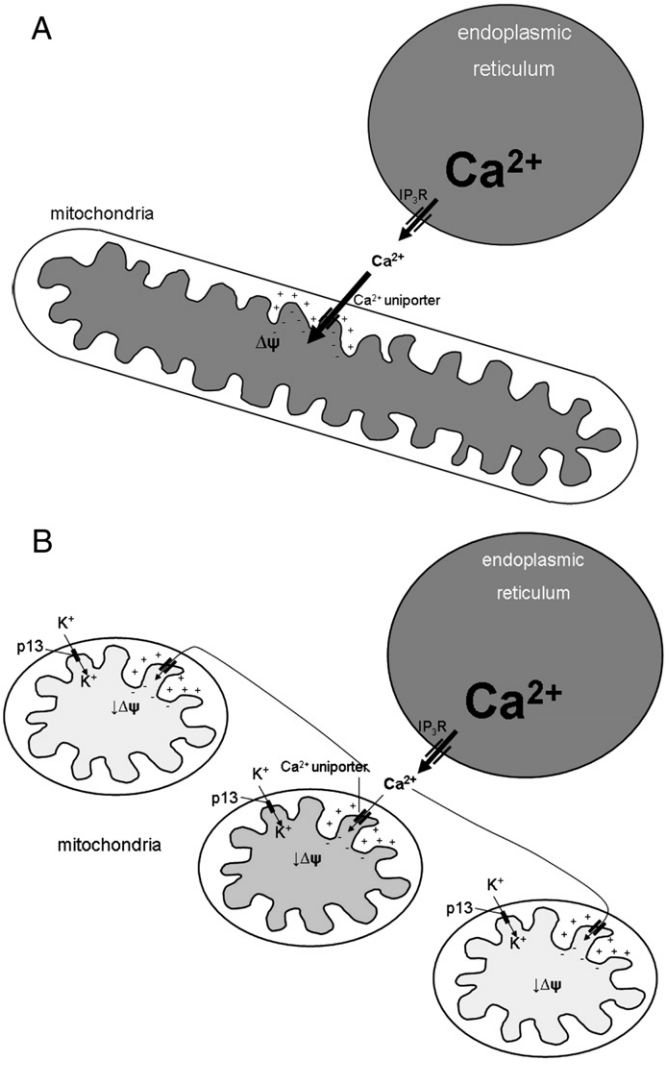

Fig. 5. Model of p13's effects on $\Delta\psi$ and Ca^{2+} uptake. (A) Under physiological conditions, Ca^{2+} released from the cellular stores is taken up by polarized mitochondria. (B) p13 induces an inward K^+ influx into the mitochondrial matrix, causing depolarization and mitochondrial fragmentation. Both these events impair mitochondrial Ca^{2+} uptake. This effect is likely to result in perturbations of intracellular Ca^{2+} homeostasis and Ca^{2+} signaling.

entry and release of viral particles [28] and is required for HCV infection in the chimpanzee model [29]. The functional properties of p7 are attributed to its ability to form a hexameric cation channel that shows selectivity for Ca^{2+} over K^+ [30] and whose activity is inhibited by amantadine [30–32] and long-alkyl chain iminosugar derivatives [32].

In a previous study, we showed that the $p13^{9-41}$ peptide (at a concentration of 5 μM) was able to change permeability to Ca^{2+} of isolated mitochondrial in a ruthenium red-independent manner [9], suggesting that this effect was not mediated through the Ca^{2+} uniporter. However, more recent studies showed that the full-length protein was unable to change the permeability of isolated mitochondrial to Ca^{2+} at a concentration (100–200 nM) that was effective on K^+ permeability and $\Delta\psi$ (V. Ciminale, unpublished observations). It is thus likely that the effects of p13 observed in living cells are mediated through its influence on mitochondrial $\Delta\psi$ and fragmentation, rather than through a direct effect on mitochondrial Ca^{2+} permeability.

It is interesting to point out that another small HTLV-1 accessory protein, p12, accumulates in the ER and Golgi [3] and interacts with calnexin and calreticulin, two ER-resident proteins that regulate Ca^{2+} storage [33,34]. This interaction results in increased Ca^{2+} release from the ER and decreases the threshold of T cell activation through NFAT transcriptional activation. These activities of p12 may explain why the protein is required for optimal viral infectivity in quiescent primary cells [34]. p12 also displays other interesting properties including association with the β and γc chains of the interleukin-2 receptor and the heavy chain of MHC class I [3]; a cleaved form of p12, named p8, accumulates at the cell surface, where it is recruited to the immunological synapse and downregulates T cell receptor signaling [35]. Thus, HTLV-1 expresses proteins that impinge on two major organelles controlling the Ca^{2+} signalsome; the possible functional interplay between p12 and p13 represents an attractive subject of future studies of HTLV-1 replication and pathogenesis.

Acknowledgments

The authors wish to thank Luigi Chieco-Bianchi, Micol Silic-Benussi, and Enrica Cannizzaro for discussions, Oriano Marin for anti-p13 antibody, and Pierantonio Gallo for graphics. This work was supported by grants from the European Union ('The role of chronic infections in the development of cancer'; contract no. 2005-018704), Istituto Superiore di Sanita AIDS research program, the Ministero per l'Università e la Ricerca Scientifica, e Tecnologica Progetti di Ricerca di Interesse Nazionale, the University of Padova (D.M.D., V.C.), the

Associazione Italiana per la Ricerca sul Cancro, the Ministero della Salute (progetto RFPS-2006-2-342010), the United Mitochondrial Disease Foundation, the Industrial Research program of the Emilia Romagna region, the Italian Multiple Sclerosis Foundation, Telethon (grant no. GGP09128), and funds from the University of Ferrara (P.P.).

References

[1] K. Verdonck, E. Gonzalez, S. Van Dooren, A.M. Vandamme, G. Vanham, E. Gotuzzo, Human T-lymphotropic virus 1: recent knowledge about an ancient infection, Lancet Infect. Dis. 7 (2007) 266–281.
[2] M. Lairmore, G. Franchini, in: K. DM, H. PM (Eds.), Human T-cell leukemia virus types 1 and 2, Fifth Edition, Fields Virology, vol. 2, Lippincott Williams and Wilkins, Philadelphia, 2007, pp. 2071–2106.
[3] C. Nicot, R.L. Harrod, V. Ciminale, G. Franchini, Human T-cell leukemia/lymphoma virus type 1 nonstructural genes and their functions, Oncogene 24 (2005) 6026–6034.
[4] R. Grassmann, M. Aboud, K.T. Jeang, Molecular mechanisms of cellular transformation by HTLV-1 Tax, Oncogene 24 (2005) 5976–5985.
[5] V. Ciminale, L. Zotti, D.M. D'Agostino, T. Ferro, L. Casareto, G. Franchini, P. Bernardi, L. Chieco-Bianchi, Mitochondrial targeting of the p13II protein coded by the x-II ORF of human T-cell leukemia/lymphotropic virus type I (HTLV-I), Oncogene 18 (1999) 4505–4514.
[6] D.M. D'Agostino, M. Silic-Benussi, H. Hiraragi, M.D. Lairmore, V. Ciminale, The human T-cell leukemia virus type 1 p13II protein: effects on mitochondrial function and cell growth, Cell Death Differ. 12 (Suppl 1) (2005) 905–915.
[7] H. Hiraragi, B. Michael, A. Nair, M. Silic-Benussi, V. Ciminale, M. Lairmore, Human T-lymphotropic virus type 1 mitochondrion-localizing protein p13II sensitizes Jurkat T cells to Ras-mediated apoptosis, J. Virol. 79 (2005) 9449–9457.
[8] M. Silic-Benussi, I. Cavallari, T. Zorzan, E. Rossi, H. Hiraragi, A. Rosato, K. Horie, D. Saggioro, M.D. Lairmore, L. Willems, L. Chieco-Bianchi, D.M. D'Agostino, V. Ciminale, Suppression of tumor growth and cell proliferation by p13II, a mitochondrial protein of human T cell leukemia virus type 1, Proc. Natl. Acad. Sci. U. S. A. 101 (2004) 6629–6634.
[9] D.M. D'Agostino, L. Ranzato, G. Arrigoni, I. Cavallari, F. Belleudi, M.R. Torrisi, M. Silic-Benussi, T. Ferro, V. Petronilli, O. Marin, L. Chieco-Bianchi, P. Bernardi, V. Ciminale, Mitochondrial alterations induced by the p13II protein of human T-cell leukemia virus type 1. Critical role of arginine residues, J. Biol. Chem. 277 (2002) 34424–34433.
[10] M. Silic-Benussi, E. Cannizzaro, A. Venerando, I. Cavallari, V. Petronilli, N. La Rocca, O. Marin, L. Chieco-Bianchi, F. Di Lisa, D.M. D'Agostino, P. Bernardi, V. Ciminale, Modulation of mitochondrial K(+) permeability and reactive oxygen species production by the p13 protein of human T-cell leukemia virus type 1, Biochim. Biophys. Acta 1787 (2009) 947–954.
[11] P. Pinton, A. Rimessi, A. Romagnoli, A. Prandini, R. Rizzuto, Biosensors for the detection of calcium and pH, Meth. Cell Biol. 80 (2007) 297–325.
[12] S. Schwartz, B.K. Felber, D.M. Benko, E.M. Fenyo, G.N. Pavlakis, Cloning and functional analysis of multiply spliced mRNA species of human immunodeficiency virus type 1, J. Virol. 64 (1990) 2519–2529.
[13] V. Petronilli, G. Miotto, M. Canton, R. Colonna, P. Bernardi, F. Di Lisa, Imaging the mitochondrial permeability transition pore in intact cells, Biofactors 8 (1998) 263–272.
[14] M. Dietel, I. Herzig, A. Reymann, I. Brandt, B. Schaefer, A. Bunge, H.J. Heidebrecht, A. Seidel, Secondary combined resistance to the multidrug-resistance-reversing activity of cyclosporin A in the cell line F4-6RADR-CsA, J. Cancer Res. Clin. Oncol. 120 (1994) 263–271.
[15] R. Rizzuto, M. Brini, P. Pizzo, M. Murgia, T. Pozzan, Chimeric green fluorescent protein as a tool for visualizing subcellular organelles in living cells, Curr. Biol. 5 (1995) 635–642.
[16] Y. Kirichok, G. Krapivinsky, D.E. Clapham, The mitochondrial calcium uniporter is a highly selective ion channel, Nature 427 (2004) 360–364.
[17] T.E. Gunter, D.I. Yule, K.K. Gunter, R.A. Eliseev, J.D. Salter, Calcium and mitochondria, FEBS Lett. 567 (2004) 96–102.
[18] P. Pinton, C. Giorgi, R. Siviero, E. Zecchini, R. Rizzuto, Calcium and apoptosis: ER-mitochondria Ca^{2+} transfer in the control of apoptosis, Oncogene 27 (2008) 6407–6418.
[19] Y. Zhou, T.K. Frey, J.J. Yang, Viral calciomics: interplays between Ca^{2+} and virus, Cell Calcium 46 (2009) 1–17.
[20] M. Chami, B. Oules, P. Paterlini-Brechot, Cytobiological consequences of calcium-signaling alterations induced by human viral proteins, Biochim. Biophys. Acta 1763 (2006) 1344–1362.
[21] A. Quintana, C. Schwindling, A.S. Wenning, U. Becherer, J. Rettig, E.C. Schwarz, M. Hoth, T cell activation requires mitochondrial translocation to the immunological synapse, Proc. Natl. Acad. Sci. U. S. A. 104 (2007) 14418–14423.
[22] S. Feske, Calcium signalling in lymphocyte activation and disease, Nat. Rev. Immunol. 7 (2007) 690–702.
[23] A.B. Parekh, Mitochondrial regulation of store-operated CRAC channels, Cell Calcium 44 (2008) 6–13.
[24] E. Majorovits, M. Nejmeddine, Y. Tanaka, G.P. Taylor, S.D. Fuller, C.R. Bangham, Human T-lymphotropic virus-1 visualized at the virological synapse by electron tomography, PloS ONE 3 (2008) e2251.
[25] H. Hiraragi, S.J. Kim, A.J. Phipps, M. Silic-Benussi, V. Ciminale, L. Ratner, P.L. Green, M.D. Lairmore, Human T-lymphotropic virus type 1 mitochondrion-localizing protein p13(II) is required for viral infectivity in vivo, J. Virol. 80 (2006) 3469–3476.
[26] H. Akl, B.M. Badran, N.E. Zein, F. Bex, C. Sotiriou, K.E. Willard-Gallo, A. Burny, P. Martiat, HTLV-I infection of WE17/10 CD4+ cell line leads to progressive alteration of Ca^{2+} influx that eventually results in loss of CD7 expression and activation of an antiapoptotic pathway involving AKT and BAD which paves the way for malignant transformation, Leukemia 21 (2007) 788–796.
[27] G. Haqshenas, J.M. Mackenzie, X. Dong, E.J. Gowans, Hepatitis C virus p7 protein is localized in the endoplasmic reticulum when it is encoded by a replication-competent genome, J. Gen. Virol. 88 (2007) 134–142.
[28] E. Steinmann, F. Penin, S. Kallis, A.H. Patel, R. Bartenschlager, T. Pietschmann, Hepatitis C virus p7 protein is crucial for assembly and release of infectious virions, PLoS Pathog. 3 (2007) e103.
[29] A. Sakai, M.S. Claire, K. Faulk, S. Govindarajan, S.U. Emerson, R.H. Purcell, J. Bukh, The p7 polypeptide of hepatitis C virus is critical for infectivity and contains functionally important genotype-specific sequences, Proc. Natl. Acad. Sci. U. S. A. 100 (2003) 11646–11651.
[30] S.D. Griffin, L.P. Beales, D.S. Clarke, O. Worsfold, S.D. Evans, J. Jaeger, M.P. Harris, D. J. Rowlands, The p7 protein of hepatitis C virus forms an ion channel that is blocked by the antiviral drug, Amantadine, FEBS Lett. 535 (2003) 34–38.
[31] S.D. Griffin, R. Harvey, D.S. Clarke, W.S. Barclay, M. Harris, D.J. Rowlands, A conserved basic loop in hepatitis C virus p7 protein is required for amantadine-sensitive ion channel activity in mammalian cells but is dispensable for localization to mitochondria, J. Gen. Virol. 85 (2004) 451–461.
[32] D. Pavlovic, D.C. Neville, O. Argaud, B. Blumberg, R.A. Dwek, W.B. Fischer, N. Zitzmann, The hepatitis C virus p7 protein forms an ion channel that is inhibited by long-alkyl-chain iminosugar derivatives, Proc. Natl. Acad. Sci. U. S. A. 100 (2003) 6104–6108.
[33] W. Ding, B. Albrecht, R. Luo, W. Zhang, J.R. Stanley, G.C. Newbound, M.D. Lairmore, Endoplasmic reticulum and *cis*-Golgi localization of human T-lymphotropic virus type 1 p12(I): association with calreticulin and calnexin, J. Virol. 75 (2001) 7672–7682.
[34] B. Albrecht, N.D. Collins, M.T. Burniston, J.W. Nisbet, L. Ratner, P.L. Green, M.D. Lairmore, Human T-lymphotropic virus type 1 open reading frame I p12(I) is required for efficient viral infectivity in primary lymphocytes, J. Virol. 74 (2000) 9828–9835.
[35] R. Fukumoto, V. Andresen, I. Bialuk, V. Cecchinato, J.C. Walser, V.W. Valeri, J.M. Nauroth, A. Gessain, C. Nicot, G. Franchini, In vivo genetic mutations define predominant functions of the human T-cell leukemia/lymphoma virus p12I protein, Blood 113 (2009) 3726–3734.